Molecular Dimensions for Adsorptives

Charles Edwin Webster,* Russell S. Drago,† and Michael C. Zerner

Contribution from the Center for Catalysis Department of Chemistry University of Florida, Gainesville, Florida 32611

Received November 14, 1997. Revised Manuscript Received March 19, 1998

Abstract: Pore volumes, accessible surface areas, and the thermodynamics of adsorption are essential in the understanding of solid surface characteristics fundamental to catalyst and adsorbent screening and selection. The recently developed Multiple Equilibrium Analysis (MEA) provides a thorough characterization of the adsorption process. Molecular properties such as molecular volumes and projected molecular areas are needed in order to convert moles adsorbed to surface volumes and probe dependent, accessible surface areas. These molecular quantities are also needed in conventional methods for determining areas and pore volumes. Generally, these molecular properties have been estimated from bulk properties, but many assumptions are required. As a result, different literature values are employed for these essential molecular properties. In this article, molecular structures for various conformers of many molecules are calculated using ZINDO. Molecular volumes and excluded molecular areas are determined from these structures and tabulated for a variety of molecules. Molecular dimensions of molecules are another important consideration needed to understand molecular exclusion as well as size and shape selectivity. Molecular dimensions along the symmetry axes are tabulated as well as the two smallest minimum dimensions of each molecule. Examples are presented to illustrate the use of these quantities in shape and size selectivity, molecular exclusion, diffusion, and adsorbent selection.

Introduction

Surface composition, area, and porosity are fundamental properties of solids that determine their suitability as adsorbents and catalyst supports. Porosity leads to shape selectivity in reactions as well as in separations, and microporosity leads to large surface areas. Surface composition influences the acidity, basicity, hydrophobicity, and hydrophilicity of the solid. Acidity, surface area, pore volume, and pore dimensions of solids are routinely described with quantitative scales, but a fundamental basis for the scales is lacking and therefore the meaning often is uncertain. Pore volumes, surface areas, and pore size distributions of solids are calculated from experimental adsorption isotherms using a variety of empirical models.[1] Pore volumes and surface areas are often quoted based on measurements with nitrogen but are adsorbate dependent quantities that depend on the pore sizes in the distribution that are accessed. For example, adsorptives larger than nitrogen may be excluded from small pores included in the nitrogen measurements. Adsorptives that give rise to specific donor−acceptor interactions result in dissimilar surface coverage when compared to those that do not.[2] Localized adsorption accompanying specific interactions (*i.e.*, one site−one adsorbate) lead to molecular orientations of the adsorptive on specific parts of the solid surface that prevent complete coverage by influencing lateral interactions between adjacent adsorbates.[3] An underestimate of the adsorbent surface area results. Even larger errors result in estimating areas when multilayer coverage occurs, and the assumption is made that there was a monolayer. Mobile adsorption gives an overestimate of the adsorbent surface area since the mean molecular occupancy is more than one molecule per surface site. The assumption is made that the adsorbed layer is liquidlike even below the saturation pressure. Criticism of this assumption arises from the application of the Clausius−Clapeyron equation to adsorption and to vapor pressure data and comparing the integration constants which do not show the correspondence of the two required by the Brunauer, Emmett, and Teller (BET) theory.[4] Finally, the BET theory assumes indefinite uptake of a saturated liquid (adsorption) over porous and planar solids. Careful measurements have shown that this adsorption is a strictly limited quantity.[5] Adamson[1] discusses the problems encountered in the calculation and empirical determination of adsorbent surface areas in detail.

For high surface area, microporous solids, traditional methods give inadequate measures of pore volumes and surface area. This insufficiency is unfortunate because microporous solids are important for efficient adsorption and for high surface area supports. Recently, a multiple equilibrium model has been proposed to interpret gas adsorption isotherms.[6,7] A series of *i*-equilibrium constants and *i*-capacities are used to characterize the minimal *i*-processes required to fit the isotherm. Each process corresponds to adsorption in a different size pore regime. The isotherms measured at several temperatures produce equi-

† Deceased, Dec 5, 1997.

(1) Adamson, A. W. *Physical Chemistry of Surfaces*; John Wiley & Sons: New York, 1990.

(2) Young, D. M.; Crowell, A. D. *Physical Adsorption of Gases*; Butterworth: London, 1962; pp 230−231. Gregg, S. J.; Sing, K. S. W. *Adsorption, Surface Area, and Porosity*; Academic Press: London, 1967; pp 68−69.

(3) Young, D. M.; Crowell, A. D. *Physical Adsorption of Gases*; Butterworth: London, 1962; p 230.

(4) Gregg, S. J.; Jacobs, J. *Trans Faraday Soc.* **1948**, *44*, 574.

(5) Gregg, S. J. *Surface Chemistry of Solids*; Reinhold: London, 1951; pp104.

(6) Drago, R. S.; Webster, C. E.; McGilvray, J. M. *J. Am. Chem. Soc.* **1998**, *120*, 538−547.

(7) (a) Drago, R. S.; Kassel, W. S.; Burns, D. S.; McGilvray, J. M.; Lafrenz, T. J.; Showalter, S. K. *J. Phys. Chem. B* **1997**, *101*, 7548. (b) Kassel, W. S.; Drago, R. S. *Microporous Materials* **1997**, *12*, 189−195.

S0002-7863(97)03906-1 CCC: $15.00
Published on Web 05/22/1998

librium constants, enthalpies, and capacities in mol per gram for each process.

With all models, knowledge of molecular dimensions is needed to convert mol of adsorbate to volumes and surface areas. Pore volume determination, mL g^{-1}, requires knowledge of molecular volumes to convert the experimental measure of mol adsorbed in units of mol g^{-1} to volume per gram. When known, the molar volume at the normal boiling point is used to make this conversion. However, reported measures of molar volumes show considerable variation. When not measured, boiling point molar volumes may be estimated both by additive methods and from critical volumes.[8] The shortcomings of these estimates have been discussed.[8]

The determination of occupied surface areas, m^2 g^{-1}, from the experimental measure of mol adsorbed in units of mol g^{-1} requires knowledge of the molecular area. Areas occupied by a molecule in a monomolecular coating have been estimated using simple drop shadow model calculations.[9] Hill[10] has derived eq 1 to calculate areas of molecules in $Å^2$ from the two-dimensional van der Waals constant, b'.

$$\text{area}_{\text{VDW}} = b' = 6.354(T_c/P_c)^{2/3} \quad (1)$$

T_c and P_c are the critical temperature (K) and pressure (atm).[10] Brunauer, Emmett, and Teller (BET) surface areas (m^2 g^{-1}) are commonly determined using a molecular area calculated from the liquid density, assuming spherical symmetry and a hexagonal close packing of the adsorbed layer. These approximations lead to the liquid density surface area, area_{LD} of eq 2 in cm^2 per molecule, where MW is the molecular mass in Daltons, N_A is Avogadro's number, and ρ is the density (g cm^{-3}) at a given temperature.

$$\text{area}_{\text{LD}}\ (\text{cm}^2) = 1.091(\text{MW}/N_A\rho)^{2/3} \quad (2)$$

Although hexagonal close packing has been the standard in the literature, other packing factors have been proposed.[11] The molecular areas that result from eq 2 are similar to the values obtained from eq 1.

Calculation of molecular volumes and areas with quantum mechanics is feasible and would have several advantages over existing compilations. The variable literature reports and different experimental estimates would be replaced by an internally consistent set of dimensions which could be calculated for new systems without recourse to time-intensive experiments. In this article, ZINDO molecular orbital calculations are carried out on a variety of molecules to produce structures from which molecular volumes, molecular areas, and critical molecular dimensions are calculated. These quantities are essential for the determination of surface areas and pore volumes as well as many other applications of porous solids including shape and size selectivity.

Calculations

ZINDO, a series of molecular electronic structure programs from the Quantum Theory Project at the University of Florida, was used to calculate molecular dimensions for both the lowest energy molecular structure and other relevant molecular conformations.[12] Implementation of the subroutine GEPOL (GEometria POLihedro, 1993) calculates the molecular surface area and the molecular volume of a molecule from the calculated structure.[13] The excluded molecular areas are calculated by projecting the shadow of the three-dimensional molecule onto a plane and connecting the outermost points. From these outermost points, an area is calculated from summing the areas of small-inscribed rectangles, similar to the application of the Trapezoidal Rule. A FORTRAN 77 program was written to calculate the excluded molecular areas in Table 2.

Results and Discussion

Pore Volumes. The porosity of a solid can be expressed in terms of a pore volume, which usually is calculated from the molar volume of an adsorbate needed to fill the pores. This measure of porosity will vary with the adsorbate, for some may be too large to fit in the smaller pores. Pore volumes from adsorbates will also differ from structural volumes because voids are created by adsorption of a molecule on one wall of a channel when the space between it and the opposite wall is too small for a second molecule. These voids lead to a lower pore volume than the structural pore volume of the solid. Our use of the term *pore volume* will refer to the volume capacity of the adsorbate, the term *structural pore volume* will be used to describe the solid's structural porosity, and *surface areas* will refer to the area of the pore or channel covered by the adsorbate.

To obtain a consistent set of adsorbate volumes for use in the conversion of mol per gram adsorbed to volume per gram, we propose to use molecular volumes determined using the GEPOL package from structures calculated with ZINDO. The calculated molecular volumes, in $Å^3$ $molecule^{-1}$, for a series of molecules are presented in Table 1 under the column labeled mVG. Converting these mVG values in $Å^3$ $molecule^{-1}$ to mL mol^{-1} produces calculated molar volumes, *M*VG, which are also presented in Table 1.

To determine the relation of these calculated values for *M*VG to experimental measurements, a correlation to experimental molar volumes, MV_{EXP} is attempted. For adsorbates that are liquid at room temperature, the molar volumes are determined from the liquid density at 25 °C and the molecular weight, *e.g.*, pentane has a density of 0.6262 g mL^{-1} that leads to a molar volume of 115.2 mL mol^{-1}. For adsorbates that are gases at room temperature, the liquid density at the normal boiling point is used in the calculation of the value used in the correlation. Over 100 polar, nonpolar, saturated, unsaturated, aromatic, and other molecules with experimental molar volumes ranging from approximately 18 (water) to 274 (tributyl phosphate) mL mol^{-1} give an excellent linear correlation to the calculated values of *M*VG shown by eq 3. It is significant that the slope of the line in eq 3 is equal to the cube of the reaction field correction factor (RFCF) of 1.2 employed by ZINDO.[14] Thus, the volume calculated from the ZINDO geometry with the reaction field correction applied gives the molar volume when converted to mL mol^{-1}.

$$MV_{EXP} = 1.7328\ M\text{VG} \quad (R^2 = 0.9797) \quad (3)$$

The liquid molar volumes, MVL, calculated from *M*VG with eq 3 are compared to the experimental values, MV_{EXP}, in Table

(8) (a) Reid, R. C.; Prausnitz, J. M.; Sherwood, T. K. *The Properties of Gases and Liquids*; McGraw-Hill: New York, 1977; pp 57−68. (b) Partington, J. R. *An Advanced Treatise on Physical Chemistry: Vol. II, The Properties of Liquids*; Longmans, Green and Co.: London, 1951; pp 17−36.

(9) McClellan, A. L.; Harnsberger, H. F. *J. Colloid Sci.* **1967**, *23*, 577.

(10) Hill, T. L. *J. Chem. Phys.* **1948**, *16: 3*, 181.

(11) Livingston, H. K. *J. Colloid Sci.* **1949**, *4*, 447. Livingston, H. K. *J. Am Chem. Soc.* **1944**, *66*, 569.

(12) Zindo, Zerner, M. C. and co-workers, Department of Chemistry, University of Florida, Gainesville, FL 32611.

(13) (a) GEPOL93; Pascual-Ahuir, J. C.; Silla, E.; Tunon, I. (b) Silla, E.; Tunon, I.; Pascual-Ahuir, J. C. *J. Comput. Chem.* **1991**, *12*, 1077.

Table 1. Molecular and Molar Volumes

compound (source[a])	density (g mL^{-1})	MW (g mol^{-1})	MV_{EXP} (mL mol^{-1})	mVG (Å^3 molc^{-1})	*M*VG (mL mol^{-1})	MVL (mL mol^{-1})	Δs^b(%)
acetone (L)	0.7908	58.08	73.45	64.447	38.81	67.25	−8.4
acetonitrile (L)	0.7868	41.05	52.17	45.943	27.67	47.94	−8.1
acetophenone (L)	1.026	120.15	117.11	120.49	72.56	125.73	7.4
ammonia (L)	0.6818	17.04	24.99	23.392	14.09	24.41	−2.3
aniline (L)	1.0217	93.13	91.15	96.448	58.08	100.64	10
anisole (L)	0.9942	108.14	108.77	108.96	65.62	113.70	4.5
benzene (L)	0.8787	78.11	88.89	85.319	51.38	89.03	0.2
benzonitrile (CRC)	1.010	103.12	102.10	102.64	61.81	107.11	4.9
benzylbromide (L)	1.438	171.04	118.94	119.3	71.84	124.48	4.7
benzyl chloride (L)	1.100	126.59	115.08	115.14	69.34	120.15	4.4
bromobenzene (CRC)	1.4950	157.02	105.03	102.12	61.50	106.56	1.5
butane (L)	0.6011	58.12	96.69	78.609	47.34	82.03	−15
2-butanone (CRC)	0.8054	72.11	89.53	81.232	48.92	84.76	−5.3
1-butene (L)	0.6255	56.10	89.69	73.288	44.13	76.48	−15
butyl acetate (CRC)	0.8825	116.16	131.63	121.95	73.44	127.25	−3.3
4-butyrolactone (L)	1.124	86.09	76.59	79.555	47.91	83.02	8.4
carbon dioxide (CRC)	1.101	44.01	39.97	34.048	20.50	35.53	−11
carbon disulfide (L)	1.2632	76.14	60.28	53.612	32.29	55.94	−7.2
carbon monoxide (L)	0.814	28.01	34.41	27.104	16.32	28.28	−18
carbon tetrachloride (CRC)	1.594	153.82	96.50	83.667	50.38	87.31	−9.5
carbon tetrafluoride (L)	1.96	88.00	44.90	48.073	28.95	50.16	12
chlorine (L)	1.5649	70.91	45.31	39.928	24.04	41.66	−8.0
chlorine monofluoride (L)	1.67	54.56	32.67	30.376	18.29	31.70	−3.0
chlorine trifluoride (L)	1.825	92.45	50.66	47.432	28.56	49.49	−2.3
chlorobenzene (CRC)	1.1058	112.56	101.79	98.478	59.30	102.76	1.0
chloroform (L)	1.484	119.39	80.45	69.944	42.12	72.99	−9.3
chloromethane (L)	0.92	50.49	54.88	42.534	25.61	44.38	−19
cyclobutane (CRC)	0.720	56.10	77.92	69.614	41.92	72.64	−6.8
cyclodecane (L)	0.871	140.27	161.04	164.34	98.97	171.49	6.5
cycloheptane (L)	0.811	98.18	121.06	116.82	70.35	121.90	0.7
cyclohexane (CRC)	0.7785	82.15	105.52	101.06	60.86	105.45	−0.1
cyclohexanone (L)	0.9478	98.15	103.56	103.63	62.41	108.14	4.4
cyclooctane (L)	0.834	112.22	134.56	133.97	80.67	139.79	3.9
cyclopentane (CRC)	0.7457	70.13	94.05	84.55	50.92	88.23	−6.2
cyclopropane (L)	0.720	42.08	58.44	54.718	32.95	57.10	−2.3
decane (L)	0.7301	142.28	194.88	179.31	107.98	187.10	−4.0
dibutyl ether (CRC)	0.7689	130.22	169.36	153.12	92.21	159.78	−5.7
2,6-di-*tert*-butylpyridine (A)	0.852	191.31	224.54	210.31	126.65	219.46	−2.3
1,2-dichlorobenzene (CRC)	1.3048	147.01	112.67	111.51	67.15	116.36	3.3
dichloromethane (CRC)	1.3266	84.93	64.02	56.301	33.90	58.75	−8.2
diethyl ether (CRC)	0.7138	74.12	103.84	87.121	52.46	90.91	−12
N,*N*-diethylformate (L)	0.908	101.15	111.40	109.42	65.89	114.18	2.5
diisopropyl ether (L)	0.7258	102.17	140.77	120.22	72.40	125.45	−11
N,*N*-dimethylacetamide (L)	0.9366	87.12	93.02	92.813	55.89	96.85	4.1
N,*N*-dimethylaniline (L)	0.9559	121.18	126.77	128.93	77.64	134.53	6.1
N,*N*-dimethylcyanamide (L)	0.867	70.09	80.84	72.154	43.45	75.29	−6.9
dimethyl ether (L)	0.661	46.07	69.70	54.012	32.53	56.36	−19
N,*N*-dimethylformamide (L)	0.9445	73.10	77.40	76.822	46.26	80.16	3.6
1,4-dioxane (L)	1.0329	88.10	85.29	84.342	50.79	88.01	3.2
diphenyl ether (L)	1.0661	170.21	159.66	163.48	98.45	170.59	6.9
dodecane (L)	0.7490	170.41	227.52	211.59	127.42	220.79	−3.0
ethane (CRC)	0.5720	30.07	52.57	45.241	27.24	47.21	−10
ethyl acetate (L)	0.9006	88.11	97.83	89.7	54.02	93.60	−4.3
ethylbenzene (L)	0.8670	106.17	122.46	118.14	71.14	123.28	0.7
ethylformate (L)	0.917	74.08	80.79	73.026	43.98	76.20	−5.7
fluorine (L)	1.513	38.00	25.11	20.737	12.49	21.64	−14
fluorine monooxide (CRC)	1.90	54.00	28.42	28.775	17.33	30.03	5.6
heptane (L)	0.6838	100.20	146.54	128.51	77.39	134.10	−8.5
hexamethylphosphoramide (CRC)	1.024	179.20	175.00	176.09	106.04	183.75	5.0
hexane (CRC)	0.6603	86.18	130.52	112.32	67.64	117.20	−10
hexyl acetate (L)	0.8779	144.21	164.27	156.45	94.21	163.25	−0.6
2,6-lutidine (L)	0.9200	107.15	116.47	113.07	68.09	117.99	1.3
methane (CRC)	0.4660	16.04	34.42	28.498	17.16	29.74	−14
methyl acetate (L)	0.9342	74.08	79.30	72.762	43.82	75.93	−4.3
N-methylimidazole (L)	1.03	82.11	79.72	82.123	49.45	85.69	7.5
4-methylpyridine (CRC)	0.9548	93.13	97.54	96.381	58.04	100.57	3.1
N-methyl-2-pyrrolidinone (CRC)	1.026	99.13	96.62	100.38	60.45	104.74	8.4
N-methylpyrrolidine (L)	0.819	85.15	103.97	96.795	58.29	101.00	−2.9
3-methylsulfonane (L)	1.191	134.20	112.68	121.61	73.23	126.89	13
naphthalene (CRC)	0.9625	128.17	133.16	128.26	77.24	133.84	0.5
nitrobenzene (CRC)	1.2037	123.11	102.28	106.86	64.35	111.51	9.0
nitroethane (L)	1.0528	75.07	71.31	67.885	40.88	70.84	−0.7
1-nitropropane (CRC)	1.0081	89.09	88.37	84.634	50.97	88.31	−0.1

Table 1. Molecular and Molar Volumes

compound (source[a])	density (g mL^{-1})	MW (g mol^{-1})	MV_{EXP} (mL mol^{-1})	mVG (Å^3 molc^{-1})	*M*VG (mL mol^{-1})	MVL (mL mol^{-1})	Δs[b](%)
nitrogen (CRC)	0.8081	28.03	34.69	23.981	14.44	25.02	−28
nitrogen dioxide (CRC)	1.4494	46.01	31.74	31.416	18.92	32.78	3.3
nitromethane (CRC)	1.1371	61.04	53.68	51.378	30.94	53.61	−0.1
nitrosyl chloride (L)	1.592	65.47	41.12	40.285	24.26	42.04	2.2
nonane (L)	0.7176	128.26	178.73	161.80	97.44	168.84	−5.5
octane (L)	0.7025	114.23	162.61	145.27	87.48	151.59	−6.8
oxygen (CRC)	1.149	32.00	27.85	22.573	13.59	23.55	−15
pentamethylbenzene (L)	0.917	148.25	161.67	165.25	99.51	172.43	6.7
pentane (L)	0.6262	72.15	115.22	95.537	57.53	99.69	−13
3-pentanone (L)	0.8143	86.13	105.77	97.744	58.86	102.00	−3.6
propane (CRC)	0.5853	44.10	75.35	61.839	37.24	64.53	−14
propionitrile (CRC)	0.7818	55.08	70.45	62.586	37.69	65.31	−7.3
propyl acetate (CRC)	0.8878	102.13	115.04	106.19	63.95	110.81	−3.7
propylbenzene (L)	0.8621	120.20	139.43	134.26	80.85	140.10	0.5
propylene carbonate (L)	1.204	102.09	84.79	87.825	52.89	91.64	8.1
pyridine (A)	0.978	79.10	80.88	79.479	47.86	82.94	2.5
quinoline (CRC)	1.0929	129.16	118.18	123.27	74.23	128.63	8.8
sulfur dioxide (CRC)	1.434	64.06	44.67	41.227	24.83	43.02	−3.7
sulfur hexafluoride (L)	1.88	146.07	77.70	73.825	44.46	77.04	−0.9
sulfur tetrafluoride (L)	1.919	108.07	56.32	56.697	34.14	59.16	5.1
sulfur trioxide (L)	1.9225	80.07	41.65	50.243	30.26	52.43	26
tetrahydrofuran (L)	0.8892	72.11	81.10	76.79	46.24	80.13	−1.2
tetrahydropyran (L)	0.8814	86.14	97.73	92.937	55.97	96.98	−0.8
tetrahydrothiophene (L)	0.9987	88.17	88.28	86.102	51.85	89.85	1.8
tetramethylene sulfone (L)	1.2614	120.17	95.27	104.67	63.03	109.22	15
1,1,3,3-tetramethylurea (L)	0.9687	116.16	119.91	121.04	72.89	126.30	5.3
thiophene (CRC)	1.0649	84.14	79.01	75.391	45.40	78.67	−0.4
toluene (CRC)	0.8669	92.14	106.29	101.32	61.01	105.73	−0.5
tributyl phosphate (L)	0.972	266.32	273.99	269.33	162.19	281.04	2.6
1,1,1-trichloroethane (CRC)	1.3390	133.42	99.64	86.526	52.11	90.29	−9.4
1,1,2-trichloroethane (L)	1.4416	133.42	92.55	86.316	51.98	90.07	−2.7
triethyl phosphate (CRC)	1.0725	182.16	169.85	170.15	102.47	177.55	4.5
1,2,4-trimethylbenzene (L)	0.8756	120.20	137.28	134.31	80.88	140.15	2.1
1,3,5-trimethylbenzene (L)	0.8637	120.20	139.17	134.14	80.78	139.98	0.6
tripropyl phosphate (A)	1.012	224.24	221.58	220.59	132.84	230.18	3.9
undecane (L)	0.7402	156.31	211.17	195.40	117.67	203.89	−3.4
p-xylene (CRC)	0.8611	106.16	123.28	117.57	70.80	122.69	−0.5
water (CRC)	0.9970	18.02	18.07	19.714	11.87	20.57	14

[a] Source of data. L: *Lange's Handbook of Chemistry*, 13th ed.; McGraw-Hill: New York, 1985. CRC: *Handbook of Chemistry and Physics*, 71st ed.; CRC Press: FL, 1991. A: *Aldrich Catalog 1994−1995*; Aldrich Chemical Co.: Milwaukee, WI, 1994. [b] $\Delta s = (100 \times (MVL - MV_{EXP})) \div MV_{EXP}$.

Table 2. Excluded Areas for Different Molecular Orientations

molecule	orientation	area (Å^2)	molecule	orientation	area (Å^2)
acetone	4 CH_3 H's	28.783	methane(2)	2 CH_4 H's	15.350[a]
benzene	6 C's	48.205	methane(3)	3 CH_4 H's	16.261
butane	2 CH_3 H's; 2 CH_2 H's	35.268	N_2	NN	15.272
chloroform	3 Cl's	34.165	NH_3	N	14.785
CO	CO	15.773	nonane	4 CH_3 H's; 6 CH_2 H's	67.588
CO(acid)	C	11.312	O_2	OO	14.655
CCl_4(2)	2 Cl's	34.314	octane	2 CH_3 H's; 6 CH_2 H's	61.477
CCl_4(3)	3 Cl's	34.017	pentane	4 CH_3 H's; 2 CH_2 H's	42.026
CO_2	OCO	19.163	propane(4a)	4 CH_3 H's	28.268
CS_2	SCS	27.293	propane(4b)	2 CH_3 H's; 2 CH_2 H's	26.812
cyclohexane	3 axial H's	47.460	propane(5)	4 CH_3 H's; 1 CH_2 H	29.596
decane	2 CH_3 H's; 8 CH_2 H's	72.944	propylbenzene	9 C's	69.525
diethyl ether	4 CH_3 H's; O	40.161	pyridine	5 C's; N	45.795
dimethyl ether	O	26.163	SF_6	3 F's	31.179[b]
ethane(3)	3 CH_3 H's	19.317	SO_2	S	20.908
ethane(4)	4 CH_3 H's	24.009	toluene	7 C's	55.346
ethylbenzene	8 C's	61.615	1,3,5-trimethylbenzene	9 C's	70.276
H_2O	O	11.130	*m*-xylene	8 C's	64.306
heptane	4 CH_3 H's; 4 CH_2 H's	55.322	*o*-xylene	8 C's	62.382
hexane	2 CH_3 H's; 4 CH_2 H's	48.623	*p*-xylene	8 C's	64.319

[a] For a tight-packed methane in this orientation, the excluded molecular area will be 13.441 Å^2. [b] For a tight-packed SF_6 in this orientation, the excluded molecular area will be 29.660 Å^2.

1 is plotted in Figure 1. The quantity Δs (Table 1) is the percent error in the calculated relative to the experimental molar volumes.

The excellent correlation of the calculated and experimental values indicates that molecular packing in the liquid phase has a minor effect on the bulk density. This is an important result,

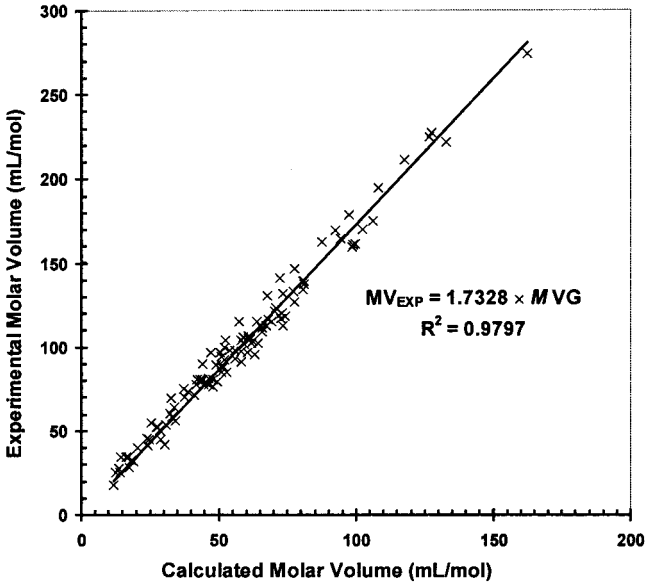

Figure 1. Correlation of the experimental molar volume, MV_{EXP}, to calculated molar volumes, *M*VG. The slope of the line is the cube of the reaction field correction factor[14] employed by ZINDO.

for it indicates that the molecular volumes are directly proportional to the molar volumes. Thus, molecular volumes can be calculated with GEPOL using a reaction field correction factor (RFCF) and converted mL mol^{-1} to give the molar volume in the liquid state without any of the conventional assumptions involving packing or molecular symmetry. With molar volumes given by density divided by molar mass, the correlation of molar volumes also implies a prediction of liquid densities.

In porosity analyses, MVL can be used to calculate the pore volume occupied by the adsorbate by converting the total moles adsorbed to a volume. For most adsorbates the occupied pore volume calculated from the mol adsorbed will be an underestimate of the structural porosity because packing of molecules smaller than the pore dimensions will result in voids. The adsorptive-dependent occupied pore volumes are relevant quantities, for they represent the volume available for the adsorptive in the solid. For a solid with fixed pore dimensions, *e.g.*, a zeolite, the most reliable estimates of the structural pore volume will come from the study of adsorbates whose dimensions are close to those of the pores, so packing will be most efficient.

Multiple equilibrium analyses, MEA, of adsorption isotherms have produced adsorption equilibrium constants (K_i) and capacities (n_i) in mol per gram for adsorption into the *i*-different groups of pore size distributions in a given solid. The smallest group of pores, with the largest equilibrium constant for binding, gives rise to process 1. Smaller equilibrium constants corresponding to groupings of larger pores are numbered consecutively. The minimum number of processes required to fit the isotherms measured at three or more temperatures is used to define the system. The pore volumes for the adsorption of six different molecules by HZSM-5, (Si/Al = 53) are obtained by summing the mmol g^{-1} for all the processes[6] and converting to volume with MVL for N_2, CO, CH_4, C_2H_6, C_3H_8, and SF_6 to yield total pore volumes of 0.071, 0.082, 0.087, 0.091, 0.099, and 0.138 mL g^{-1}, respectively, show that the capacities depend on the adsorbate. SF_6, the probe closest to the dimensions of the HZSM-5 pore, produces the highest calculated pore volume. These calculations are in accordance with the view that probe molecules smaller than the pore dimensions give rise to voids in filling the HZSM-5 channels. The calculated micropore volume from Harkins-Jura *t*-plots is 0.14 mL g^{-1}, which is in excellent agreement with the result from SF_6 adsorption.

(14) A common scaling of all van der Waal radii by 1.2 is used in most reaction field models to give good energies of solvation as well as excitation energies. The cube of this, 1.728, might be compared with the empirically determined slope of 1.733 of eq 3.

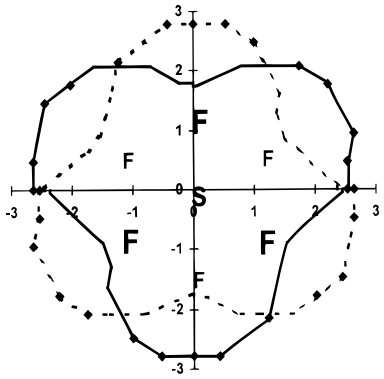

Figure 2. Illustration of the excluded molecular area. The SF_6 molecule is chosen to illustrate the projection of a surface bound molecule onto a planar surface. The molecule is arranged to maximize surface interaction. The dashed line outlines the surface bound fluorines illustrated with a large F and the solid line those on the opposite face of the octahedron illustrated with a small F. The solid diamonds outline the projected area.

Surface Areas. Conversion of moles g^{-1} adsorbed in a monolayer to area g^{-1} produces the accessible solid surface areas for the different adsorbates. For adsorbates undergoing nonspecific interactions, the calculated *molecular* area is determined by the projection of the molecule onto a plane. This calculated area is termed the excluded molecular area. The geometry of the adsorbate on the surface will influence the amount covering the surface and needs to be predicted to calculate the area occupied by an adsorbate molecule. The conformation of the molecule may not necessarily be the same as the minimum energy structure in the gas state or even in solution. For a nonpolar adsorptive, the predicted conformation is the one that maximizes surface contact, with ambiguities resolved by selecting the conformation expected to maximize dispersion interactions. However, the energy change to the predicted conformation from the minimum energy structure must only be a few kcal mol^{-1}, so that the net interaction is more exothermic than that of simply binding the minimum energy structure. For example, an ethane molecule, with the carbon−carbon bond parallel to the surface, can interact with the surface with four hydrogens of an eclipsed conformation or with three hydrogens of the minimum energy staggered conformer. The energy cost of 2.8 kcal mol^{-1} to give the eclipsed conformation would have to be provided by an increase in the surface interaction for the eclipsed compared to the staggered form. In view of the ambiguity in the selection of geometries, excluded molecular areas with the RFCF applied are presented in Table 2 for the minimum energy conformation and other orientations of the adsorbate molecule on the surface. The calculation of excluded molecular area is illustrated for the SF_6 molecule in Figure 2.

For monolayer adsorption, the process capacities in mmol g^{-1} can be converted to surface areas by knowing the molecular area of an adsorbate for the molecular configuration involved in the adsorbate−adsorbent interaction. The process capacities from the MEA of HZSM-5 are summed and converted to surface areas for N_2, CO, CH_4, C_2H_6, C_3H_8, and SF_6. The resulting values are 260, 260, 285, 278, 273, and 335 m^2 g^{-1}, respectively.

The value for SF_6 is calculated assuming an open structure in which the molecules adsorb as shown in Figure 3a with no

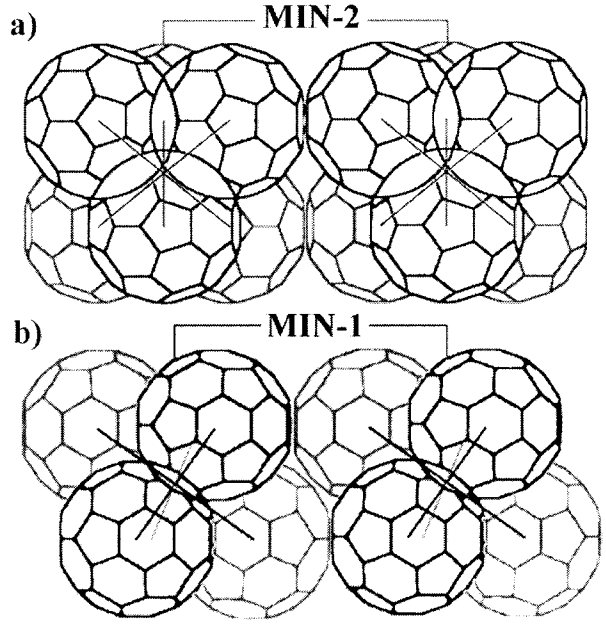

Figure 3. Illustration of surface adsorbed SF_6 (a) loose packed and (b) tight packed. In (a), the straight lines define the orientation of the octahedron and point to all six fluorines of which all six are visible in this orientation. The two molecules shown are separated by MIN-2. In (b), the straight lines define the orientation of the octahedron and point to all six fluorines of which only four are visible in this orientation. The two molecules shown are separated by MIN-1.

overlap of the excluded area. Tighter packing is possible in which the top triangle of fluorines of one molecule overlaps the bottom triangle of another, *e.g.*, a second SF_6 molecule approaches the first molecule along the *y*-axis or similarly the diagonal of Figure 3b. Tighter packing is expected because of increased intermolecular dispersion interactions with no loss in adsorbate−surface interactions and leads to an area of 319 m^2 g^{-1}.

Ethane in the staggered conformation with three hydrogens interacting or in the eclipsed conformation with four hydrogens interacting have the same area when the C−C bond is parallel to the surface. An ethane molecule could interact in a staggered conformation with the C−C bond perpendicular to the surface. Three hydrogens would interact with one wall of the channel and to a lesser extent**,** three with the distant wall. This orientation is ruled out in HZSM-5 because the resulting surface area would only be 223 m^2 g^{-1}. More ethane would be adsorbed in the experiment if this were the orientation of the adsorptive. Thus, the free energy gained by adsorbing more molecules and packing more ethane into the pores does not compensate for the free energy lost in rearranging fewer ethane molecules interacting with the C−C bond parallel to the surface.

Methane was calculated in a conformation with the three hydrogens of the face of the tetrahedron flat on the surface. In HZSM-5, methane could pack with two hydrogens interacting with the surface. Since this orientation leads to a weaker surface interaction and a tight-packed area of 235 m^2 g^{-1}, the calculated surface areas distinguish the two possibilities.

Propane could interact with the surface through five hydrogens (two from each CH_3 and one from CH_2), four hydrogens (from the two CH_3 groups), or four hydrogens (two from methyl and two from CH_2). Areas of 273 m^2 g^{-1}, 261 m^2 g^{-1}, and 248 m^2 g^{-1}, respectively result. The conformation involving four hydrogens from methyl and methylene groups can be ruled out because of the low surface area calculated. These examples illustrate the added insight into the adsorption process that results from determining adsorbate dependent areas.

These adsorbent surface areas are probe dependent quantities because the accessibility of the solid's porosity will depend on the minimum dimensions of the adsorptive (vide infra). Even if a given adsorbate molecule experiences interactions with opposite pore walls (in pores with molecular dimensions), the calculated adsorbent surface area has an inherent accessibility dependence. In a study of the MEA of Na-mordenite,[15] the calculated surface areas demonstrate this probe accessibility dependence quite clearly. Since the side channel of the mordenite structure is only accessed by the smaller adsorptives (N_2, CO, etc.), there is a three-process description of adsorption, while larger adsorptives only have a two-process description of adsorption (for adsorption in the main channel). The calculated surface areas for N_2 and CO are approximately 350 m^2 g^{-1}, while the larger adsorptives (CH_4, C_2H_6, SF_6, etc.) have calculated surface areas progressively less than 265 m^2 g^{-1}. Therefore, while a given solid could have pores that are of molecular dimensions, the calculated surface area will show this accessibility dependence for adsorptives of similar minimum dimensions (vide infra). At this point, it should be noted that the calculated surface area alone cannot discriminate pores of molecular dimension from those greater than molecular dimensions. The excluded area of a given probe only describes the area taken by its projection onto a plane. However, since the probe dependent, occupied pore volume represents a three-dimensional occupancy, the calculated pore volume will not be conditional on the ratio of the pore dimension to the adsorptive dimension.

The calculated accessible surface area is by necessity and definition the area excluded by the adsorptive molecules in a plane. An increase in the calculated pore volumes will represent a decrease in the ratio of pore diameter to effective molecular diameter, but only when the pore diameter is less than two molecular diameters. In the case where the pore diameter becomes less than two molecular diameters, by definition, the calculated accessible surface area does not change.

In the case where two or more populations of pores are present for which the diameters are near that of the adsorptive molecule, these pore regimes would be resolvable with an MEA study. For example, in the HZSM-5 study, the two pores of the structure that are very close in dimensions are resolved by the description of the adsorption process, which MEA provides. If not resolvable, these pores would calculate a given capacity, n_i (more than likely, with a larger error), and therefore one surface area.

The areas from liquid density and the McClellan's average areas[9] (from probe molecules which were measured more than five times, independently) correlate well to each other, R^2 of 0.974. These areas differ significantly from those in Table 2, especially for long chain and cyclic hydrocarbons. Our concern, the area of the solid occupied, is for a molecular configuration that maximizes the dispersion contribution and not necessarily the configuration the molecule has in the liquid state. For example, it has been reported that long chain hydrocarbons adsorbed to a surface are elongated to maximize dispersion interactions.[16]

The data in Table 2 should find wide application in surface area determination. Different cross sections for complex molecular structures can be calculated and information gained

(15) Cottone, A.; Webster, C. E.; Drago, R. S. To be submitted.
(16) June, R. L.; Bell, A. T.; Theodorou, D. N. *J. Phys. Chem.* **1990**, *94*, 1508.

Table 3. Molecular *x*, *y*, *z*, MIN-1 and MIN-2 Dimensions

molecule	*x*	*y*	*z*	MIN-1	MIN-2
acetone	6.600	4.129	5.233	4.129	5.233
benzene	6.628	7.337	3.277	3.277	6.628
butane	7.855	4.519	4.014	4.014	4.519
chloroform	6.181	5.713	4.613	4.613	5.713
CCl_4	6.207	5.723	5.748	5.723	5.748
CO	3.280	3.339	4.182	3.280	3.339
CO_2	3.339	3.189	5.361	3.189	3.339
CS_2	3.535	3.376	6.655	3.376	3.535
cyclohexane	7.168	6.580	4.982	4.982	6.580
decane	15.319	4.538	4.014	4.014	4.538
diethyl ether	4.027	8.822	4.556	4.027	4.556
2,6-di-*tert*-butylpyridine	11.344	6.454	8.294	6.454	8.294
dimethyl ether	4.083	6.319	4.127	4.083	4.127
ethane	3.809	4.079	4.821	3.809	4.079
ethylbenzene	6.625	5.285	9.361	5.285	6.625
H_2O	3.226	2.917	3.888	2.917	3.226
heptane	11.589	4.523	4.014	4.014	4.523
hexane	10.344	4.536	4.014	4.014	4.536
2,6-lutidine	8.927	4.127	6.957	4.127	6.957
methane	3.829	4.101	3.942	3.829	3.942
N_2	3.054	2.991	4.046	2.991	3.054
NH_3	3.697	3.989	3.111	3.111	3.697
nonane	14.076	4.524	4.014	4.014	4.524
octane	12.833	4.537	4.014	4.014	4.537
O_2	2.985	2.930	4.052	2.930	2.985
pentane	9.101	4.522	4.014	4.014	4.522
propane	6.606	4.516	4.020	4.020	4.516
propylbenzene	6.625	5.277	10.274	5.277	6.625
pyridine	6.648	3.339	6.475	3.339	6.475
SF_6	6.270	6.182	6.321	4.871	5.266
SO_2	4.227	3.365	5.462	3.365	4.227
toluene	6.625	4.012	8.252	4.012	6.625
1,2,3-trimethylbenzene	9.058	4.062	8.227	4.062	7.635
1,2,4-trimethylbenzene	7.576	4.024	9.145	4.024	7.251
1,3,5-trimethylbenzene	8.276	8.553	4.062	4.062	8.178
m-xylene	8.994	3.949	7.315	3.949	7.258
o-xylene	7.269	3.834	7.826	3.834	7.269
p-xylene	6.618	3.810	9.146	3.810	6.618
HD[a]	9.923	5.098	6.076	5.098	6.076
VX[b]	12.719	9.192	7.804	7.804	9.192
sarin (GB)[c]	8.299	6.763	6.690	5.622	5.794
soman (GD)[d]	9.731	8.152	7.247	6.991	7.247

[a] 2,2′-Dichlorodiethyl sulfide. [b] *O*-Ethyl S-2-(diisopropylamino)ethyl methylphosphonothiolate. [c] 2-Propyl methylphosponofluoridate. [d] 3,3-Dimethyl-2-butylmethylphosphonofluoridate.

about adsorbate binding configuration. Furthermore, in a solid whose area is known, the number of mmol of a new adsorbate taken up by the solid can be estimated from the adsorbates surface area. This estimate requires that the molecular dimensions of the new adsorbate and the adsorbate used to determine the solids area permit access to the same pores.

Critical Dimensions. Knowledge of the dimensions of molecules is essential to understanding molecular exclusions as well as shape and size selectivity in zeolites.[17] Table 3 contains the dimensions of the molecule along the *x*, *y*, and *z* symmetry axes of the molecule calculated for each atom surrounded by a van der Waal sphere, without the reaction field correction factor of 1.2. The dimension of the adsorbate that is critical for entry into a pore will depend on the shape of the pore. For example, in slit-shaped pores the size of the adsorptive in the minimum dimension**,** MIN-1, will determine if the molecule can enter the pore (see Figure 4a). This direction can be determined by rotating the molecule to find an axis which represents the minimum distance through the molecule. In cylindrical pores, the size of the molecule in two directions must be considered. The relevant dimensions are MIN-1 and the next to the smallest perpendicular distance for low energy conformations or molecular orientations that enable a molecule to enter

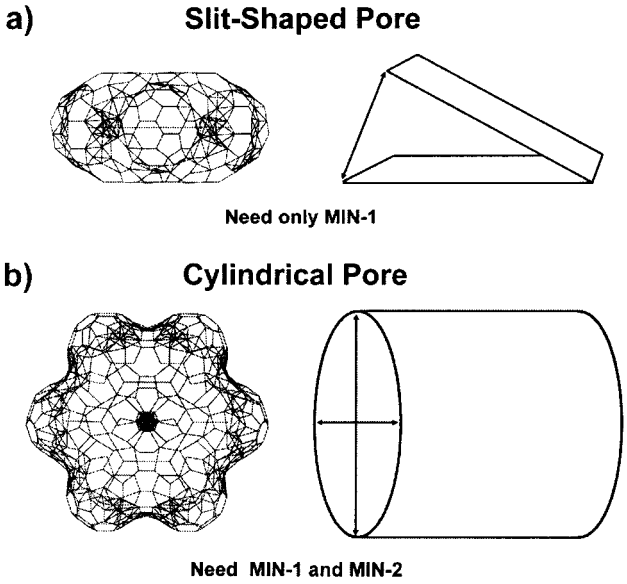

Figure 4. Application of the MIN-1 and MIN-2 of a benzene adsorptive molecule to pore access. The minimum dimensions of the adsorptive dictate pore access. In (a), MIN-1 less than the dimension of a slit-shaped pore is required for access. In (b), MIN-1 and MIN-2 less than the two dimensions of a cylindrical pore is required for access.

a cylinder, MIN-2 (see Figure 4b). Table 3 contains the MIN-1 and MIN-2 dimensions of molecules that are relevant to size and shape selectivity considerations. The MIN-1 and MIN-2 distances are specified for each molecule with each atom surrounded by a van der Waal sphere, without the reaction field correction. For example, pentane and hexane are elongated cylinders with approximately the same minimum critical dimensions since they have the same cross sectional diameter.

The critical dimensions reported in Table 3 are in accord with experimental observations attributed to shape selectivity.[18] Shape selectivity in HZSM-5 by MAS NMR showed that when 1,2,3-, 1,3,5-, and 1,2,4-trimethylbenzene (MIN-2 of 7.64, 8.18, and 7.25 Å, respectively) were all produced inside in the 9 Å channel intersections of HZSM-5, only 1,2,4-trimethylbenzene is obtained as a product.[18] Only this isomer is small enough to exit through the channels,[19] and the others rearrange to reestablish equilibrium between those remaining in the pores. Additionally, a previous report from our laboratory concluded that the strongest Brønsted acid sites reside in the smaller straight channels of HZSM-5.[20] Pyridine interacted with the strongest sites in the solid to produce an enthalpy of -42.1 kcal mol^{-1}. 2,6-Lutidine could not access these strongest sites, and the largest enthalpy was -19.0 kcal mol^{-1}. Pyridine has a smaller critical dimension of 6.43 Å, compared to 2,6-lutidine with 6.95 Å. With a critical dimension of 8.29 Å, 2,6-di-*tert*-butylpyridine cannot access either channel. This denied access was manifested in the calorimetric measurements with 2,6-di-*tert*-butylpyridine by a small negative enthalpy from a small number of hydrogen bonding sites residing on the exterior of HZSM-5. For more discussion on the determination of effective catalytic pore sizes see ref 19.

Kinetic diameters or Lennard-Jones potentials constants, σ_k, have been employed to determine the accessibility of molecules

(17) (a) Csicsery, S. M. *Zeolites* **1984**, *4*, 202. (b) Csicsery, S. M. *Pure Appl. Chem.* **1986**, *58*, 841.

(18) Anderson, M. W.; Klinowski, J. *J. Am. Chem. Soc.* **1990**, *112*, 10−16. Anderson, M. W.; Klinowski, J. *Nature* **1989**, *339*, 200.

(19) Webster, C. E.; Drago, R. S.; Zerner, M. C. Submitted to *J. Phys. Chem. B.*

(20) Drago, R. S.; Diaz, S.; Torrealba, M.; de Lima, L. *J. Am. Chem. Soc.* **1997**, *119*, 9, 4444.

to zeolite channels and are related to the minimum equilibrium diameter of a molecule, r_{min}, given by a Leonard-Jones 12−6 potential, i.e., $r_{min} = 2^{1/6}\sigma_k$,[21] and assume the molecule is effectively spherical. Kinetic diameters do not take into account molecular orientation, and this orientation is crucial in determining whether a molecule will fit into a small pore of fixed size.[22] For large, nonspherically symmetrical molecules, kinetic diameters will not be useful in determining whether the molecule can enter a pore. Thus, the critical dimensions reported here should be considered as a better criterion of molecular exclusion.

It is of interest to determine the relation of Breck's kinetic diameters[23] as well as Svehla's kinetic diameters[24] to our calculated values of MIN-1 and MIN-2. The correlation coefficients (R^2) for MIN-1 are 0.656 and 0.744 and for MIN-2 are 0.623 and 0.837, respectively. From these results, one can conclude that reported kinetic diameters at best provide estimates of the critical molecular dimensions that determine access to a pore.

The next concern is to determine if the reported kinetic diameters have any physical significance. This was evaluated by calculating a molecular volume for the assumed spherically symmetric molecule from the reported kinetic diameter and comparing the volume to mVG. The correlation coefficient (R^2) is 0.882 for Svehla's diameters and is 0.781 for Breck's diameters. Thus, one can conclude that MIN-1 and MIN-2 provide a more realistic measure of molecular access.

In the absence of specific interactions, molecular dimensions are relevant to diffusion. Diffusivities (D) of a series of *n*-alkanes are reported[25a] in HZSM-5. With comparable values of MIN-1 and MIN-2 for long chain alkanes in the elongated conformer expected on solids, MIN-3 will be the controlling factor. The correlation produced the equation: $\ln D = -0.525$ (MIN-3) − 12.9 with an R^2 of 0.986 (MIN-3 is the *z*-axis for ethane and *x* for longer chain hydrocarbons). Methane is left out of the correlation and deviates in the direction of diffusing too rapidly. This is expected behavior for the Knudsen diffusion found for methane compared to configurational diffusion[25b] of higher alkanes.

General Applications. To illustrate the utility of the methods presented above in adsorbent design and selection, the adsorption of chemical warfare agents (CWA)[26] are discussed. A ZINDO calculation was carried out on Mustard, VX, Sarin, and Soman molecules. The conversion of these results to MVL gave 130.5, 274.4, 127.7, and 181.0 mL mol^{-1} respectively. The excellent agreement of these calculated values with experimental values of 124.9, 265.2, 127.1, and 178.2 mL mol^{-1} provides confirmation of eq 3. The critical dimensions of these molecules indicate that microporosity 7 Å or less will not be utilized for adsorption. Furthermore, for mustard and VX adsorptives, adsorbents with slit shaped pores will be more effective than those with cylindrical pores because MIN-2 is much larger than MIN-1 for these molecules. In evaluating adsorbents for CWA's, simulant molecules are more convenient to work with than the agents. In selecting compounds to model nonspecific adsorption of agents, molecules with similar critical dimensions should be employed. Molar volumes of the simulants and agents can be compared to estimate adsorbent capacities.

Conclusions

The comparison of experimental molar volumes (MV_{EXP}) to molar volumes calculated with ZINDO (*M*VG) yields an excellent correlation (see eq 3 and Figure 1) confirming the feasibility of the quantum mechanical calculation of molar volumes and densities. Since the calculated molar volumes correlate to experimental molar volumes without regard to molecular packing, the MVL values in Table 1 are the best quantities for the conversion of mmol adsorbed per gram to volume adsorbed per gram.

Physical surface characteristics can be explored with the application of the molecular volumes and the projected molecular surface areas (Table 2 and Table 3) derived from the molecular dimensions. Pore volumes and areas can be calculated for a given adsorbent from the moles adsorbed. Adsorbent surface areas calculated for various conformers of the adsorptive are shown to provide insights into the packing of the adsorbate in the pores or channels of the solid.

Knowledge of the molecular dimensions of adsorptive molecules is crucial to the understanding of molecular exclusion, as well as shape and size selectivity. The critical molecular dimensions (Table 3) are used to explain molecular exclusions of adsorptives from a solid (*e.g.*, shape selectivity in the synthesis of alkyl-benzenes and exclusion of 2,6 di-*tert*-butylpyridine from HZSM-5) and diffusivity of alkanes in porous solids (*e.g.*, zeolites).

Acknowledgment. The authors would like to thank Edgewood Research, Development, and Engineering Center (ERDEC), the Army Research Office (ARO), and the Office of Naval Research (ONR) for financial support as well as additional funding from an IBM SUR Grant.

JA973906M

(21) Hill, T. L. *An Introduction to Statistical Thermodynamics*; Addison-Wesley: Reading, MA, 1960; p 484.

(22) Breck attempted to include molecular orientation in some of the molecules. listed, e.g., *n*-butane has a smaller σ_k than propane as determined from both viscosity data or second virial coefficients. Therefore, Breck quoted the σ_k of butane as the same as propane. The minimum dimension (MIN-1) for propane and butane are the same, the difference is in MIN-2. MIN-2 in this article is quoted for an elongated butane. Although an elongated butane has less steric strain than a "cis"-butane, the elongated conformer has a larger apparent diameter.

(23) Breck, D. W. *Zeolite Molecular Sieves*; John Wiley & Sons: New York, 1974; p 636.

(24) Reid, R. C.; Prausnitz, J. M.; Sherwood, T. K. *The Properties of Gases and Liquids*; McGraw-Hill: New York, 1977; pp 678−679.

(25) (a) Hayhurst, D. T.; Paravar, A. *Zeolites*. **1988**, *8*, 27. (b) Chen, N. Y.; Degnan, T. F., Jr.; Smith, C. M. *Molecular Transport and Reaction in Zeolites*; VCH Publishers: New York, 1994; pp 81−86.

(26) Yang, Y. C.; Baker, J. A.; Ward, J. R. *Chem. Rev.* **1992**, *92*, 1729.